AGU PUBLICATIONS

JGR

Journal of Geophysical Research: Space Physics

RESEARCH ARTICLE
10.1002/2016JA023797

This article is a companion to *Dougherty et al.* [2017] doi:10.1002/2017JA024053 and *Bodisch et al.* [2017] doi:10.1002/2017JA024148.

Key Points:
- Voyager plasma data are reanalyzed using model constraints on ion composition
- Net charge density and ion temperatures are basically consistent with previous analysis
- Small regions of cold plasma with varying composition are found in the plasma sheet

Correspondence to:
F. Bagenal,
bagenal@colorado.edu

Citation:
Bagenal, F., L. P. Dougherty, K. M. Bodisch, J. D. Richardson, and J. M. Belcher (2017), Survey of Voyager plasma science ions at Jupiter: 1. Analysis method, *J. Geophys. Res. Space Physics*, *122*, doi:10.1002/2016JA023797.

Received 21 DEC 2016
Accepted 14 MAR 2017
Accepted article online 17 MAR 2017

Survey of Voyager plasma science ions at Jupiter: 1. Analysis method

F. Bagenal[1], L. P. Dougherty[1], K. M. Bodisch[1], J. D. Richardson[2], and J. M. Belcher[2]

[1]Laboratory for Atmospheric and Space Physics, University of Colorado Boulder, Boulder, Colorado, USA, [2]Center for Space Research, Massachusetts Institute of Technology, Cambridge, Massachusetts, USA

Abstract The Voyagers 1 and 2 spacecraft flew by Jupiter in March and July of 1979, respectively. The Plasma Science instrument (PLS) acquired detailed measurements of the plasma environment in the equatorial region of the magnetosphere between 4.9 and 4 R_J. While bulk plasma properties such as charge density, ion temperature, and bulk flow were reasonably well determined, the ion composition was only well constrained in occasional regions of cold plasma. The ion data obtained by the PLS instrument have been reanalyzed using physical chemistry models to constrain the composition and reduce the number of free parameters, particularly in regions of hotter plasma. This paper describes the method used for fitting the plasma data and presents the results versus time. Two companion papers describe the composition of heavy ions and present analysis of protons plus other minor ions.

1. Introduction

The 4 July 2016 arrival of NASA's Juno spacecraft at Jupiter heralds a new phase of exploration of Jupiter's magnetosphere and marks an appropriate time to summarize previous plasma observations at Jupiter. Overviews of the structure of the magnetosphere are provided by *Khurana et al.* [2004] and *Krupp et al.* [2004] as well as by the more recent review of *Bagenal et al.* [2014] in the context of observations to be made by Juno. *Bagenal et al.* [2016] present a reanalysis of data from the Galileo plasma instrument [*Frank et al.*, 1992] and a survey of plasma disk temperature, density, and flows, while Galileo orbited Jupiter between December 1995 and September 2003. *Nerney et al.* [2017] review ultraviolet observations of ion composition in the Io plasma torus from Voyager, Galileo, and Cassini missions. In a series of three companion papers we present a reanalysis of Voyagers 1 and 2 Plasma Science (PLS) data obtained at Jupiter in March and July 1979, respectively. In this paper 1 we summarize the data and our analysis technique. In paper 2 [*Dougherty et al.*, 2017] we present the ion composition found in different regions of the Jovian plasma disk. In paper 3 [*Bodisch et al.*, 2017] we discuss the distribution of protons and other minor ion species. An additional purpose of this paper is to document a public archiving of the Voyager PLS data from Jupiter and computer codes for processing them (http://lasp.colorado.edu/home/mop/missions/voyager).

Each of the Voyager spacecraft carries a set of Faraday cups, three of which (A, B, and C cups) measure ions, a fourth (D cup) measures both ions and electrons, in the energy-per-change range of 10 to 5950 V. These Voyager Plasma Science (PLS) instruments are described in detail by *Bridge et al.* [1977] and discussed further in section 2 below. The PLS observations of electrons at Jupiter are discussed by *Scudder et al.* [1981] and *Sittler and Strobel* [1987]. We concentrate on the ion observations in this paper and present a summary of previous analyses of Voyager PLS ion data below. Note that the PLS Faraday cups separate the inflowing ion species according to their energy-per-charge. Thus, multiple ion species that have a common bulk speed are separated by their mass-to-charge (M/Z) ratio. If the plasma has a relatively fast flow and low temperature (i.e., the flow is supersonic), then the different ion species produce separately resolved peaks in the energy-per-charge spectra. For transsonic or subsonic flows the peaks of the different ion species merge together. A quirk of nature has further frustrated analysis of ion composition at Jupiter: the two dominant ion species, S^{++} and O^{+}, share the same M/Z ratio of 16 (amu per unit charge).

The initial results from the March 1979 Voyager 1 flyby of Jupiter is presented by *Bridge et al.* [1979a], listing the multiple spacecraft crossings of the bow shock (11) and magnetopause (5) and highlighting the first in situ detection of sulfur and oxygen ions of different ionization states. While optical emissions from neutral sodium and S^{+} ions associated with Io had been observed from Earth (see review by *Thomas et al.* [2004]),

the density and variety of ionization states were not appreciated until the Voyager 1 ultraviolet spectrometer (UVS) instrument detected intense ultraviolet emissions from the torus of plasma outside Io's orbit [*Broadfoot et al.,* 1979]. The initial report of PLS results from the July 1979 Voyager 2 flyby listed 12 crossings of the bow shock and 18 crossings of the magnetopause (perhaps suggesting a more variable solar wind during the second flyby) and emphasized the presence of regions of cold plasma in the middle magnetosphere [*Bridge et al.,* 1979b].

Subsequent analysis of PLS data can be separated into discussions of the Io plasma torus [*Sullivan and Bagenal,* 1979; *Bagenal et al.,* 1980; *Bagenal and Sullivan,* 1981; *Bagenal,* 1985] and debates about the flow in the plasma sheet [*McNutt et al.,* 1979, 1981; *Belcher et al.,* 1980; *Belcher and McNutt,* 1980]. The total plasma content of magnetic flux tubes (constructed from radial profiles of density and temperature) shows a dramatic drop inside Io's orbit (into the cold, inner torus) and a relatively flat profile in the dense, hot, outer torus. These profiles of flux tube content (NL^2) were interpreted by *Richardson et al.* [1980] and *Richardson and Siscoe* [1981, 1983a] in terms of relatively rapid outward transport of plasma via centrifugally driven flux tube interchange and much slower (by a factor of 50 to 100) inward transport driven (as in Earth's plasmasphere) by turbulence at the end of the flux tubes in the planet's atmosphere/ionosphere. When trying to model profiles of NL^2 and ion temperature with radial diffusion models, *Richardson and Siscoe* [1983b] found it difficult to reconcile the inferred transport timescale (25–100 days) with the total power radiated (~2 TW) and observed electron temperature (~5 eV). We return to this topic in our discussion of our newly derived ion temperature profiles in paper 2.

A review of the post-Voyager description of the thermal plasma in the Jovian magnetosphere is presented by *Belcher* [1983]. *McNutt* [1983, 1984] extended his analysis of the middle magnetospheric plasma with an assessment of the force balance in the plasma disk where he concluded that a component of outward force (opposing the magnetic field confinement) seems to be lacking. It was around this time that the Voyager PLS team at Massachusetts Institute of Technology found there had been a coding error in the analysis of PLS data in the Io plasma torus and previously published torus temperatures needed to be increased by a factor of 2 [*Bagenal et al.,* 1985]. In further analysis of the inner torus, *Bagenal* [1985] used the density, composition, and ion temperature inside Io's orbit to derive the latitudinal distribution of plasma. Otherwise, the PLS team was busy with data from the Saturn (Voyager 1 in November 1980 and Voyager 2 in August 1981) and Uranus (January 1986) flybys.

In the regions of cold plasma (the inner torus, small pockets of the plasma sheet) where the plasma has a high Mach flow that enters approximately normal to each sensor, the PLS instrument response can be simply approximated with an effective area. To evaluate plasma conditions where the flow is transsonic or subsonic, it was clear that a more sophisticated approach was needed for the PLS instrument response. *Barnett and Olbert* [1986] developed an instrument response for the four cups that allowed for oblique and subsonic flows. *Barnett* [1986] used the new instrument response to analyze the flow near Io, flow that *Belcher et al.* [1981] and *Belcher* [1987] interpreted in terms of Io generating Alfven wings that carry 3×10^6 A of electrical current. It is the instrument response of *Barnett and Olbert* [1986] that we use in this study (see section 2).

One topic that theorists struggle with understanding is the scale on which centrifugally driven interchange is being driven. *Richardson and McNutt* [1987] looked at the currents into the Voyager PLS sensors at the highest temporal resolution (*L* modes) and found that on 0.24 s timescale (which translates to an effective spatial resolution of ~20 km), the density does not fluctuate more than 20% (more typically $<5\%$). These observations ruled out theories (such as proposed by *Pontius et al.* [1986] and *Summers and Siscoe,* 1985) that required interchange of full and (essentially) empty flux tubes. An alternative driving mechanism for radial transport was proposed by *McNutt et al.* [1987] who argued that the ballooning instability (that occurs in plasmas of finite plasma β and on much smaller scales) might be responsible. They examined some regions of plasma depletions that occurred on the Voyager 2 flyby between 13 and 17 R_J (radius of Jupiter = 71,492 km) that others had ascribed to Ganymede [*Burlaga et al.,* 1980].

Another topic that occupies theorists' attention is the dynamics of the outer plasmasheet—how much is driven by internal dynamics versus ionosphere-magnetosphere coupling versus external solar wind fluctuations? *Sands and McNutt* [1988] expanded on the *Barnett and Olbert* [1986] instrument response to include the effects of temperature anisotropy to derive the plasma flow field in Jupiter's dayside middle

magnetosphere (10–25 R_J). They found nonazimuthal flows tended to be aligned (or antialigned) with the magnetic field, perhaps as the magnetosphere responds to changes in solar wind dynamic pressure. The *Sands and McNutt* [1988] study also puts limits on the thermal anisotropy of $T_{||}/T_{\perp} < 3$ in the plasma sheet and showed that, in reality, the additional complexity they added to the instrument response was not necessary. We have therefore not included thermal anisotropy in our study.

In the cold, inner torus the plasma flow is sufficiently supersonic that the ion composition could be reasonably well determined [*Bagenal,* 1985]. Even the $M/Q = 16$ peak could be determined to be mostly O^+, to be at a common temperature with the other ion species, consistent with the long transport times and low electron temperatures. But in the warm, outer torus and much of the plasma sheet the ion spectra have overlapping peaks and analysis of the PLS ion data required making assumptions about the composition, often based on ultraviolet emission lines from the brightly emitting torus. The *Bagenal et al.* [1992] study of torus composition combined analysis of in situ PLS data with Voyager UVS data analyzed by *Shemansky* [1988]. This combined composition analysis became the basis of an empirical model of the Io plasma torus by *Bagenal* [1994] that was applied extensively to subsequent studies of the Jovian magnetosphere. Part of the discussion about the ion composition revolves around the observation that the ionization state of the ions seems to increase with distance and that the total emitted power (~2 TW) requires an additional source of hot (say ~50–100 eV) electrons [*Moreno et al.,* 1985; *Shemansky,* 1988; *Barbosa,* 1994]. *McNutt et al.* [1990] argued that the suprathermal electrons in the PLS electron measurements [*Scudder et al.,* 1981; *Sittler and Strobel,* 1987] could be backscattered from energetic particles precipitating into Jupiter's atmosphere (where they excite auroral emissions).

The Cassini spacecraft flyby of Jupiter (with a primary goal of gaining a gravity assist to Saturn) provided an excellent opportunity to study UV emissions from the Io plasma torus between October 2000 and March 2001 [*Steffl et al.,* 2004a]. *Steffl et al.* [2004b] showed that spectral analysis of the torus emissions suggested the ion composition was very different at the Cassini epoch than at the time of Voyager. Recent analysis by *Nerney et al.* [2017] of the Voyager UVS data using the most recent atomic data for emission rates suggests an ion composition more consistent with the UV emissions observed in the Cassini era and with models of the torus physical chemistry matched to the Cassini UV data [*Delamere et al.,* 2005].

This paper presents a survey of ion data obtained by the Voyager PLS instrument in the Jovian magnetosphere which is reanalyzed using constraints based on recent reanalysis of Voyager UVS data [*Nerney et al.,* 2017] and modeling of the physical chemistry of the Io plasma torus [*Delamere et al.,* 2005]. The paper is structured as follows: in section 2 we describe the Voyager PLS instrument and how the instrument response varied along the Voyager 1 and Voyager 2 trajectories through the Jovian system. Section 3 describes the ion energy-per-charge spectra and how we fit them with multiple ion species assuming comoving isotropic Maxwellian functions. In section 3.4 we present the resulting plasma properties obtained along the spacecraft trajectories which are compared with previous analyses. We present our conclusions in section 4.

2. Instrument and Response

2.1. PLS Instrument

The Plasma Science (PLS) experiment on the Voyagers 1 and 2 spacecraft comprises four modulated-grid Faraday cups (see *Bridge et al.* [1977] for complete instrument description). The main sensor consists of three sensors (A, B, and C cups) which are symmetrically arranged and tilted ~20° away from an axis that is parallel to the spacecraft high-gain antenna (usually pointed toward the Earth). The side sensor (D cup) is ~88° from the main sensor symmetry axis, roughly opposite the A cup normal.

Currents due to positive ions are measured simultaneously in all four cups across the energy-per-charge range of 10 to 5950 V. The D cup also measures currents due to electrons over the same energy-per-charge range. This voltage range is covered by discrete, continuous bins, spaced approximately logarithmically. The ion measurements utilize two instrument modes: a low-resolution mode with 16 voltage steps with $\Delta E/E \sim 29\%$ (*L* mode); and a higher-resolution mode with 128 voltage steps with $\Delta E/E \sim 3.6\%$ (*M* mode). Electrons are measured via E1 and E2 modes which cover low-energy (10 to 140 eV) and high-energy (140 to 5950 eV) electrons, each in 16 contiguously spaced channels with $\Delta E/E \sim 10\%$ for E1 and $\Delta E/E \sim 29\%$ for E2.

During the Jupiter encounter a complete *L* and *M* modes took 3.84 and 30.72 s to acquire, respectively. Each measurement sequence took 96 s during which currents from an *L* mode plus either the first or last 72 channels of an *M* mode are telemetered to Earth. It takes two measurement sequences (192 s) to cover the full energy-per-charge range of an *M* mode.

For our analysis of *M* modes we alternate between summing channels (1–72 + 73–128) then the next time step summing channels (1–56 + 57–128). This means that there can be a discontinuity between channels 56–57 or 72–73, but it does allow the highest temporal resolution.

2.2. Response Function

This study uses the response of the Voyager PLS sensors derived by *Barnett and Olbert* [1986] and applied by *Barnett* [1986]. The response function of the cup is defined as the ratio of the particle flux reaching the collector to the particle flux incident on the aperture when the incident particles are a collimated, monoenergetic beam, and the response function is calculated by studying the trajectories of the particles inside the cup. The response function can be written as a product of two terms: the "sensitive area" and the grid transparency. The sensitive area term is computed from a straightforward study of the trajectories, while statistical arguments are required to determine the grid transparency term. This response assumes each component of the plasma comprises a convected Maxwellian velocity distribution. For low ion temperatures (i.e., supersonic flows), the response function can be modeled as a simple Gaussian function. For higher ion temperatures (i.e., subsonic or transsonic flows), the response is more complicated. While *Sands and McNutt* [1988] adapted the Barnett response function for a plasma with a thermal anisotropy, we assume that the plasma is isotropic in this study.

The primary effect of the Barnett response on an incoming Maxwellian beam is to spread the signal to lower energies. The hotter (lower Mach number) the plasma, the more currents are spread. The Barnett response seems to work well for flow angles up to about 55° for the side sensor and up to 70° for the main sensors. Plasma parameters derived for more oblique flows require more complex response (e.g., as used by *Sands and McNutt* [1988]).

2.3. Spacecraft Trajectories and Instrument Response to a Corotating Beam of Plasma

During the flybys, Voyager 1 reached a closest approach at 4.9 R_J, while Voyager 2 came within 10 R_J of the planet. Figure 1 shows the trajectories of the two spacecraft and the corresponding responses of the PLS Faraday cups to a cold corotating beam of plasma. The response for each cup is calculated as the fraction of flow that is directly normal to the surface of the Faraday cup (positive V_Z in the frame of the sensor). Therefore, this cold-beam response can be given as follows:

$$R = V_z/|V|.$$

A response of 1 indicates that the flow is completely into Faraday sensor, while a value of 0 means that the flow is perpendicular to the sensor. The abrupt changes in the response curves are due occasions where the spacecraft changed attitude to accommodate a mission activity. The symmetry axis (S) of the main sensors (A, B, and C cups) is parallel to the communication antenna and usually pointed toward the Earth (and close to the direction of the Sun). On approach to Jupiter the side sensor (D cup, perpendicular to S) is pointed toward the corotational direction. Around closest approach the flow comes into the main sensor. After closest approach the corotational flow moves out of the PLS field of view until a roll maneuver that puts the flow back into the D cup. Unfortunately, these roll maneuvers happened too far away from the planet to obtain significant fluxes on the outbound passes.

The plasma in the Jovian magnetosphere is not uniform in density nor necessarily flowing in the corotational direction so this response function does not guarantee where there will be strong plasma measurements. Note that there are also a few places where we are missing pointing information. Fortunately, these are not places where we have good data.

3. Data and Fitting

3.1. PLS Data

Early presentations of Voyager PLS data showed three-dimensional spectrograms as shown in Figure 2a which illustrates the change (sometimes rapid) in the nature of energy-per-charge spectra with time as the

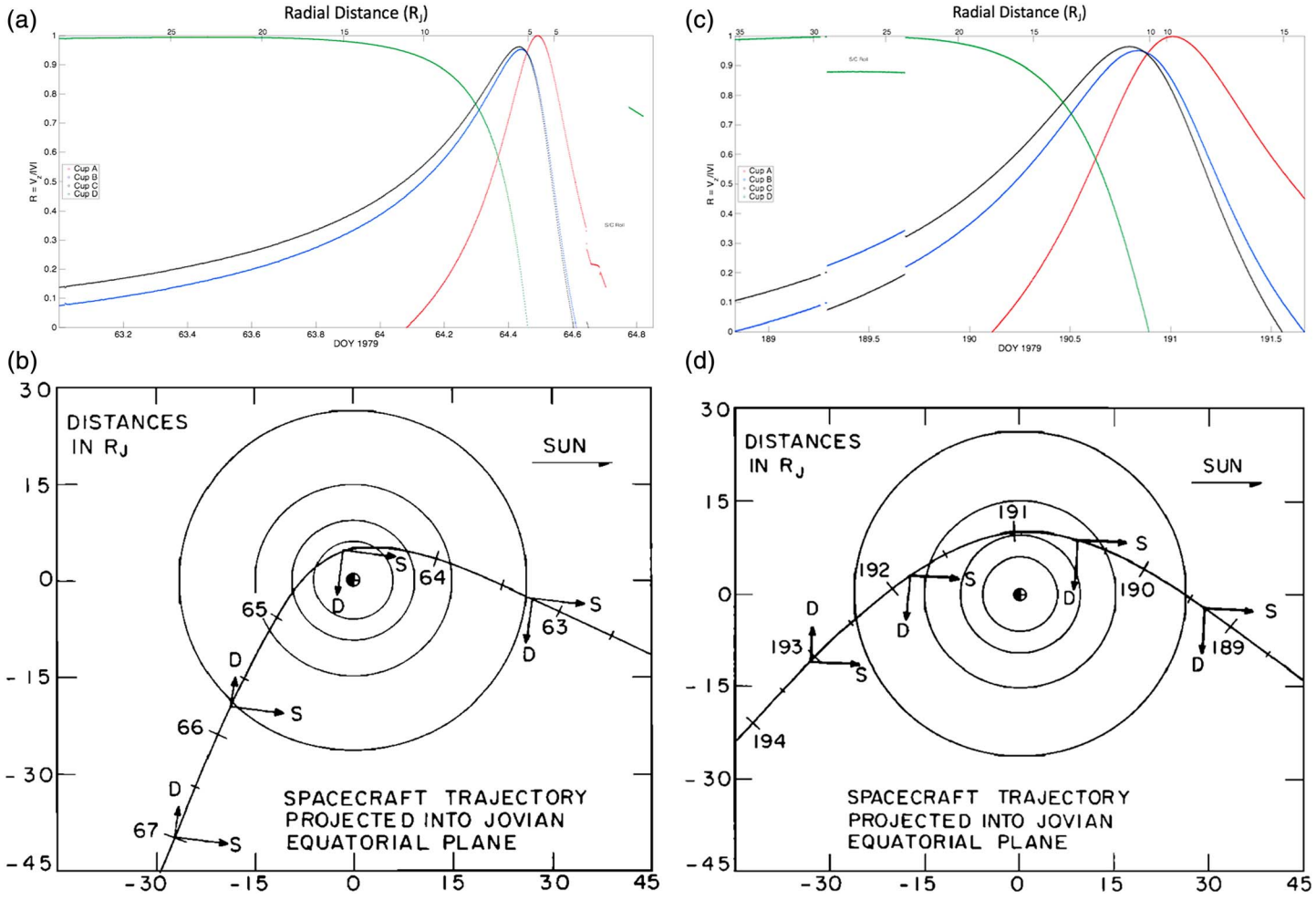

Figure 1. (a) Response of the Voyager 1 Faraday cups to a cold beam of corotating plasma. (b) The trajectory of the V1 through the Jovian system with the orbits of Io, Europa, Ganymede, and Callisto. The arrows point in the direction of the D cup and the symmetry axis (*S*) for A, B, and C cups. (c and d) Same as Figures 1a and 1b but for Voyager 2.

spacecraft moves from warm plasma (where the spectral peaks are merged) to cold regions where the spectral peaks for different ions are separated. The example in Figure 2a also illustrates how the protons sometime pop up above the background at low energies. The modern method is the color spectrogram in Figure 2b that shows data from all four ion sensors in *M* modes as well as the E1 and E2 electron data from the D cup. These data were taken on day of year (DOY) 64 1979 from Voyager 1 with the closest approach to Jupiter occurring in the middle of the day. Various sources of instrumental noise can be observed in these color spectrograms (e.g., vertical lines) that we have colored gray. There are also instrumental effects that appear as horizontal lines in the main sensors (the notches in the spectra shown in Figures 3b and 3c).

The changing geometry shown in Figure 1a is revealed by the higher fluxes in the D cup at the beginning of the day, moving into the main sensor as the spacecraft moved through the warm, then cold, torus regions, and persisting in the A cup. As the spacecraft receded from Jupiter on the nightside the corotational flow moved out of the PLS fields of view and only the (subsonic) electrons produce significant flux, into the D cup. At ~1800 h the spacecraft rolled, bringing corotational flow briefly back into the D sensor.

At each flyby of Jupiter there were approximately 20,000 *L* and *M* mode spectra taken by the Voyagers 1 and 2 PLS instruments within the magnetosphere. For many of these spectra the measured fluxes were too low or they were severely noise limited. In this reanalysis of the data we have limited our fits to 770 Voyager 1 (between mid-DOY 63 to mid-DOY 65) and 103 Voyager 2 (DOY 190 and 191) spectra, mostly *M* modes.

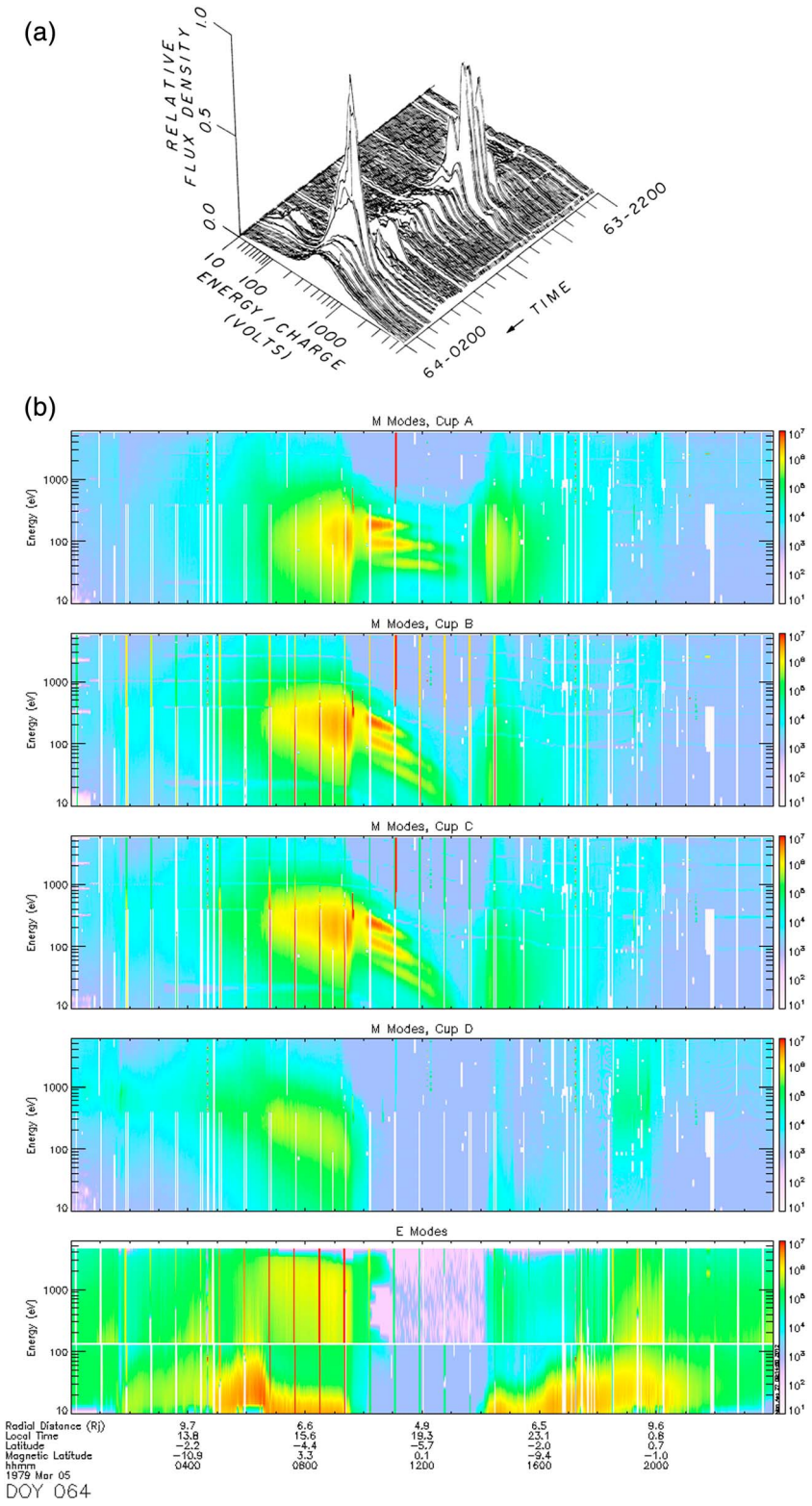

Figure 2. (a) Voyager 1 energy-per-charge spectra obtained with the D cup on the inbound pass between ~33 R_J and ~11 R_J. From *McNutt et al.* [1981]. (b) Voyager 1 energy-per-charge versus time spectrogram for ion *M* modes in the A, B, C, and D cups plus the electron E1 and E2 modes in the D cup. The data were taken on DOY 64 between 13 R_J and 4.87 R_J with closest approach to Jupiter around midday. The scale of the color bar is current in fA.

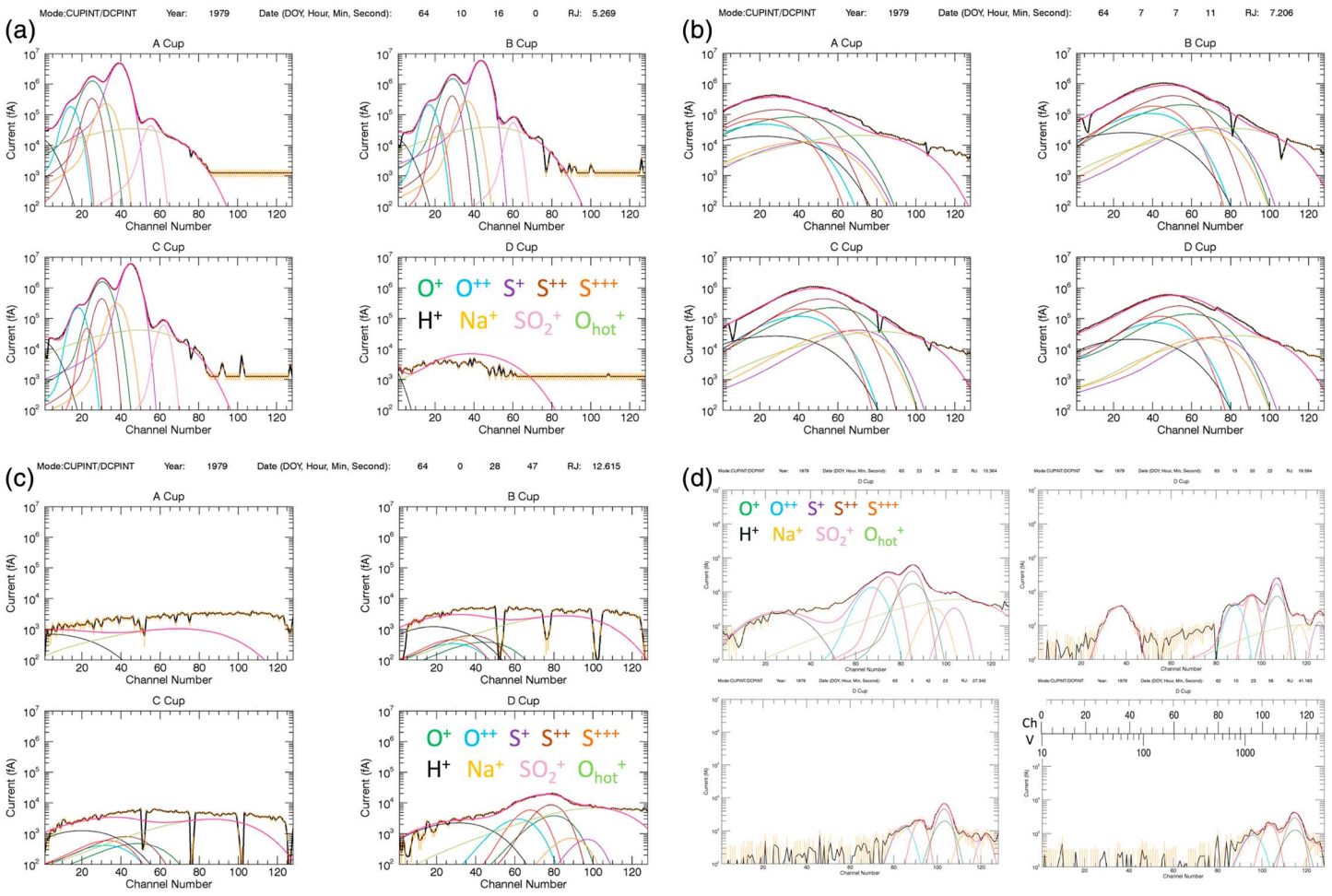

Figure 3. (a) Voyager 1 spectra fitted with parameter regimes corresponding to case i (all parameters allowed to vary). (b) Voyager 1 spectra fit with parameter regimes corresponding to case iii (Delamere composition and corotation). (c) Voyager 1 spectra fit with parameter regimes corresponding to case ii (Delamere composition, variable flow). (d) Voyager 1 spectra fitted with parameter regimes corresponding to case iv (composition modified from Delamere). We have added a channel number to *E/q* (in volts) conversion scale.

3.2. Error in PLS Measurements

The Voyager PLS instrument measures a current (I) due to a flux of charged particles into the sensor. The PLS team use units of femptoamps (fA) and typical observed M mode currents at Jupiter range from a minimum of ~10^3 fA (10^{-12} A) to ~10^7 fA (10^{-8} A). The signal in the *L* modes also had a minimum level of ~10^3 fA. On Voyager 1 the *L* mode currents hit saturation at 10^6 fA between about 0600 and noon. Luckily, this dense region of the torus is where the *M* modes have good signal. The *L* modes also saturated briefly on the outbound pass through the warm torus before a spacecraft maneuver turned the PLS instrument away from the corotating flow. The *L* mode gain was set lower on the Voyager 2 flyby so there were no saturated spectra on the second pass.

The measurement error (in fA) used in the original analysis of the PLS data combined in quadrature a background error and a measurement error:

$$\begin{aligned} \text{Error}^2 &= \text{Error}^2_{\text{Background}} + \text{Error}^2_{\text{Measurement}} \\ &= 54 + 1.118 \times 10^{-4} I^2 \end{aligned}.$$

After examining several spectra throughout the magnetosphere of Jupiter, we found that a more realistic estimate of the errors to be as follows:

$$\begin{aligned} \text{Error}^2 &= \text{Error}^2_{\text{Background}} + \text{Error}^2_{\text{Measurement}}. \\ &= 10^4 + 2.5 \times 10^{-5} I^2 \end{aligned}$$

This puts the background signal at about 100 fA and the measurement error at 0.5%. More detailed discussion of PLS data errors is presented in the online documentation (http://lasp.colorado.edu/home/mop/files/2015/06/Voyager-PLS-Error-Analysis.pdf).

Figure 3 shows some sample *M* mode spectra to illustrate the range of cases we have analyzed. The above error formula has been applied to the data as gold error bars. They become noticeable when currents drop below about 10^4 fA.

3.3. Fitting Method

The goal of this study is to pull as much information out of the Voyager PLS data as possible, folding in additional information about the Jovian magnetospheric plasma that has emerged since the original analysis. We fit the spectra with as complete a set of plasma parameters as possible but when there are limited features in the spectra we add further constraints. We assume the ions are comoving convected Maxwellian functions parameterized by a common flow velocity plus a density and temperature for each ion species, allowed to vary separately or constrained as necessary. When the ions are cold, each ion can be clearly distinguished and when there are resolved data in at least three sensors we uniquely fit all three components of the velocity. Outside the inner cold torus region, the temperatures either became too large and the spectral peaks merged or the flow only produced significant signal in the D cup so that nonazimuthal components (in the V_R and V_Z directions) could not be uniquely determined. Under such circumstances it is necessary to either make assumptions about the composition to determine the flow, or vice versa. Our priorities in this paper are the composition and azimuthal flow. A more extensive discussion of nonazimuthal flows in Jupiter's middle magnetosphere are given by *McNutt et al.* [1981] and by *Sands and McNutt* [1988].

Most of the spectra fell into distinct cases described below with a few examples that required a combination of methods. We used the MPFIT reduced chi-square minimization technique [*Markwardt*, 2009] to find the best match to the spectra, checking each spectrum to see if the fit looked reasonable. Sometimes, further simplifications were made to the model and fewer parameters were allowed to vary. There were only two common simplifications. The first was to only vary the density of O^+, while all other ion species were set as a ratio to that parameter, effectively varying only the total density. These ion composition ratios were determined from the physical chemistry model of the torus derived by *Delamere et al.* [2005] to match the radial profile of UV emissions observed by the Cassini Ultraviolet Imaging Spectrograph (UVIS) instrument [*Steffl et al.,* 2004b]. Second, in the regions that the Delamere composition model did not match, we used an interpolation between well fitted data and the Delamere model. We describe these specific cases below.

3.3.1. The O^+ and S^{++} Ambiguity

Deriving ion composition at Jupiter is plagued by that fact that both O^+ and S^{++} have the same *M*/*Q* value of 16. Because of this ambiguity, and due to the fact that the current measured is proportional to both density and the charge, it is possible to fit the data with a linear superposition of the two species.

This $M/Q = 16$ ambiguity forced us to constrain the density of S^{++} to a fixed fraction of the O^+ density. From their physical chemistry model of the Io plasma torus *Delamere et al.* [2005] show that the ion composition converges by ~9 R_J to a density ratio of $O^+/S^{++} \sim 1.2$, the value we used throughout the middle magnetosphere. Between 9 and 6 R_J, the chemistry model suggests that the O^+/S^{++} ratio slightly increases from 1.2 to 1.3 and then rapidly increases inside 5.7 R_J. Inside the inner cold torus ($<5.3\ R_J$) the charge state of the ions plummets and we assumed that the S^{++} density was likely not more than 10% of O^+. We took a linear interpolation between $O^+/S^{++} = 1.3$ and 10 in the transition region from 6 to 5.3 R_J.

3.3.2. Cases

We illustrate typical spectra for various different cases in Figures 3a–3d. The resulting ion parameters are shown in Table 1.

3.3.2.1. Case I: Variation of All Parameters

An illustration of such a case is shown by the fit to the spectra in Figure 3a. In this method of fitting, all of the parameters are allowed to vary. This technique is used mainly in the cold torus, where the density of ions is high and the temperatures low. In the cold torus, the full flow vector could be determined but the plasma flow was very close to corotation and nonazimuthal components of the flow were very small. In general, seven to nine parameters were fit in this region for Voyager 1 data obtained between 64:10:07 and

Table 1. Ion Properties Derived for Spectra Shown in Figures 3a–3d[a]

	64—10:16	64—07:07	64—00:28	63—23:34	63—15:50	63—05:42	62—10:23
Time	Figure 3a Case i	Figure 3b Case iii	Figure 3c Case ii	Figure 3d Case iv	Figure 3d Case iv	Figure 3d Case iv	Figure 3d Case iv
R_J	5.269	7.206	12.615	13.364	19.594	27.342	41.183
N_e	1859 ± 1.4%	772 ± 0.6%	10 ± 5.3%	14.2 ± 2.7%	2.0 ± 7.8%	0.6 ± 16%	0.3 ± 24%
H^+	4.3	17.7	1.0	0.91 ± 0.2%	0.26 ± 23%		
H^+/N_e %	0.23	2.3	10	6.4	13		
O^{++}	21 ± 0.001%	42	0.4	0.8 ± 0.2%	0.1 ± 11%	0.04 ± 30%	0.02 ± 100%
O^{++}/N_e%	1.1	5.4	3.8	5.7	5.0	6.7	6.4
O^+	376 ± 0.001%	177 ± 0.001%	1.0 ± 0.6%	2.2 ± 0.2%	0.34 ± 11%	0.13 ± 30%	0.07 ± 100%
O^+/N_e %	20	23	10	15	17	22	22
S^{+++}	2.4 ± 0.01%	40	0.38	0.8 ± 0.2%	0.09 ± 11%	0.03 ± 30%	0.02 ± 100%
S^{+++}/N_e %	0.1	5	3.8	5.6	4.5	5.1	6.4
S^{++}	38	140	0.85	1.8	0.29	0.11	0.06
S^{++}/N_e %	2.0	18	8.5	13	14	19	19
S^+	1227 ± 0.001%	28	0.13	0.3 ± 0.2%	0.04 ± 12%	0.03 ± 30%	
S^{++}/N_e %	66	4	1	2	2	5	
O^+_{hot}	50	37	4	2.9	0.28		
$O_{hot}{}^+/N_e$ %	2.7	4.8	40	20	14		
Na^+	66 ± 0.001%	28	0.16	0.35 ± 0.2%	0.04 ± 80%	0.04 ± 200%	0.02 ± 600%
Na^+/N_e %	3.6	3.7	1.6	2.4	2.0	7.3	7.4
$SO_2{}^+$	9.0 ± 0.002%						
$SO_2{}^+/N_e$ %	0.48						
T (H^+)	4.4	100 ± 1%	60 ± 24%	21 ± 9%	3.8 ± 100%		
Ti	2.2 ± 1%	100 ± 1%	60 ± 24%	21 ± 9%	16.7 ± 20%	22.1 ± 40%	36.8 ± 60%
T_{hot}	127	575	750	750	900		
V_{phi}	66.0 ± 0.1%	90.5	118 ± 1.4%	133 ± 0.4%	188 ± 0.4%	175 ± 1.2%	216 ± 1.8%
V_{phi}/V_{co}	1.00	1.00	0.74	0.79	0.77	0.51	0.42

[a]Units: Densities are in cm^{-3}, temperatures are eV, velocities are in km/s, and abundances are ni/N_e*100. The percent abundance relative to charge density is shown in blue. The percent uncertainties in the fit parameters are shown in green.

64:13:32: T_i, V_φ, V_R, V_Z, and density of the following species: O^+, O^{++}, S^{+++}, S^+, and $SO_2{}^+$. Sometimes, a clear signal of H^+ could be fit at the low limit of energy/charge (see discussion on fitting protons below). The regions where this case applied are colored blue in Figures 4b and 5b.

3.3.2.2. Case II: Delamere Composition

Applying a physical chemistry model between 6 and 9 R_J, *Delamere et al.* [2005] derived the mixing ratios for the primary charge states of oxygen and sulfur ion: O^+, O^{++}, S^+, S^{++}, and S^{+++}. An illustration of such a case is shown in Figure 3b. Outside 9 R_J, the density of the plasma has become sufficiently tenuous that collisions cease and the composition of the plasma $>9\,R_J$ is frozen in (Figure 8 of *Delamere et al.* [2005] shows that most reaction timescales exceed transport timescales $>8\,R_J$). In the PLS data, we found this to be mostly true, though we made some small adjustments occasionally. Inside 6 R_J, this composition broke down and a linear interpolation of the composition was used between 6 R_J and 5.3 R_J (the case I method above) and worked well in fitting the data. On few occasions, one ion would be present in unusually high concentration so it would be allowed to vary freely to more accurately model the data (discussed further in paper 2). In general, three parameters were fit in this region: n, T_i, and V_φ. The regions where this case applied are shown with red bars in Figures 4b and 5b.

3.3.2.3. Case III: Delamere Composition With Fixed Flow Speed

Between 6 and 7.5 R_J on the inbound approach of Voyager 1, the plasma reached a consistent temperature of around 100 eV, which was slightly hotter than the surrounding regions. Due to the anticorrelation between temperature and flow speed, the fitting procedure managed to find better mathematical fits by reducing the flow speed and greatly increasing the temperature. The resulting parameters were unphysical, the temperature values between 0.5 and 4 KeV. To constrain the solutions, the flow speed was constrained to rigid rotation. Given that this region is still well before the observed break in corotation at 10 R_J, we feel confident in forcing corotation. In general, two parameters were fit in this region: n and T_i, and an illustration of such a case is shown in Figure 2c. The regions where this case applied are colored black in Figures 4b and 5b. Note that the notches in some of the spectra are due to spacecraft activities that vibrate the grids in the

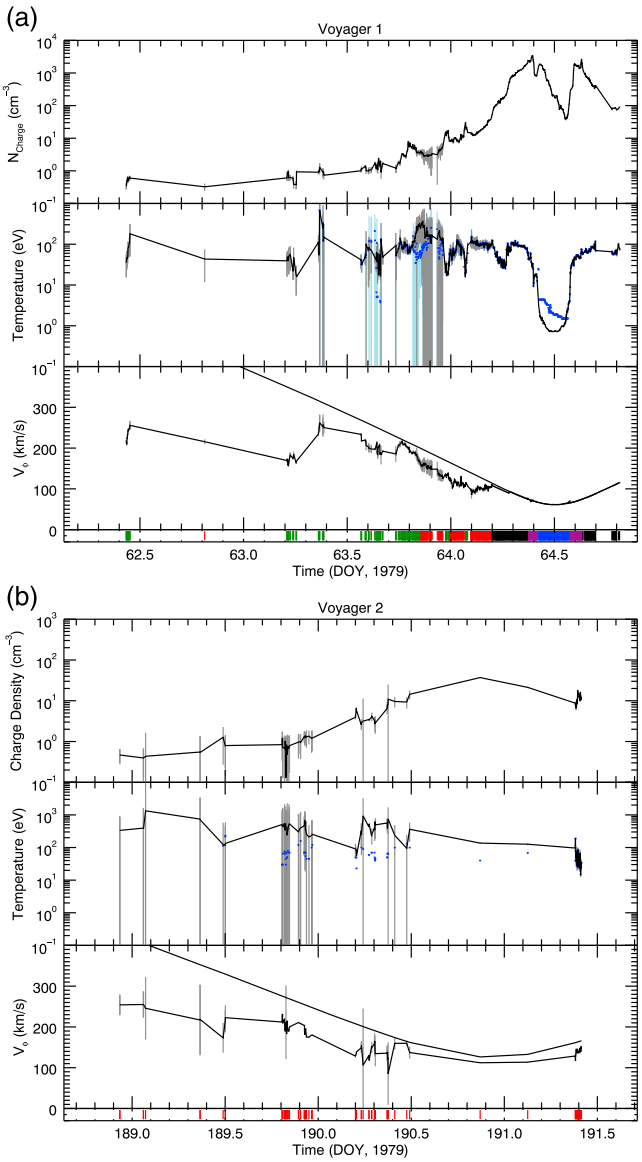

Figure 4. Density, temperature (black for heavy ions and blue for protons), and azimuthal flow derived from fitting (a) Voyager 1 and (b) Voyager 2 spectra. The colors in the bottom strips show the type of fit that was applied (case i in blue, case ii in red, case iii in black, case iv in green, and case v in purple). The smooth curve shows local rigid corotation.

Faraday cups. At the time of the spectra in Figure 3c the direction of the corotational flow was transitioning from the D cup into the main sensor (A, B, and C cups) as illustrated in Figure 1a. The angle of the flow into the A (particularly), B, and C cups is sufficiently large that the instrument response used in our analysis is not reliable. In fitting spectra like that in Figure 3c we paid little attention to the fit to the A, B, and C spectra and focused on the data obtained in the D cup.

3.3.2.4. Case IV: Cold Blobs

Throughout the magnetosphere, there are several regions where the plasma ions decrease in temperature compared to the surrounding plasma—"cold blobs." The composition in these cold blobs varies, suggesting they may have a rather different origin than the surrounding plasma. Due to the freezing in of the ion composition beyond ~9 R_J, many of these plasmoids do have a similar composition but it is difficult to locate their origin. For these, at least three parameters were fit: n, T_i, and V_φ. For some of these, a particular ion species was prevalent enough to allow fitting of that density uniquely, thus avoiding compositional constraints. Illustrations of such cases are shown in Figure 3d. The regions where this case applied are colored green in Figures 4b and 5b.

3.3.2.5. Case V: Hot-Cold Transition

Finally, there are a few cases inside of 6 R_J where the peaks are not well defined but the plasma abundance is clearly changing between the hot torus composition (consistent with *Delamere et al.*'s [2005] physical chemistry model) to the resolved composition of the cold torus inside ~5.2 R_J. For these spectra we interpolated the composition between these 6 and 5.2 R_J. The corresponding regions where this technique is applied have bars colored purple in Figure 4b.

3.3.3. Fitting H^+ Ions

Protons appear regularly throughout the magnetosphere of Jupiter. Unlike the dissociation products of SO_2 from Io's volcanoes, there are multiple potential sources of protons: the solar wind, the ionosphere of Jupiter, or dissociation and ionization of water from the icy moons. We find that in general, protons make up 10–30% of the total charge density in the magnetosphere, usually closer to 10% than 30%. The protons have more variable temperatures. In some regions, protons have a similar temperature to the heavy ions, and in other regions they follow a different temperature profile. Also, due to their low mass, low charge state, and their relatively low density, the signal from protons is usually weaker and closer to the level of noise in the PLS instrument. This meant that the automated fitting routine sometimes increased the temperature of the

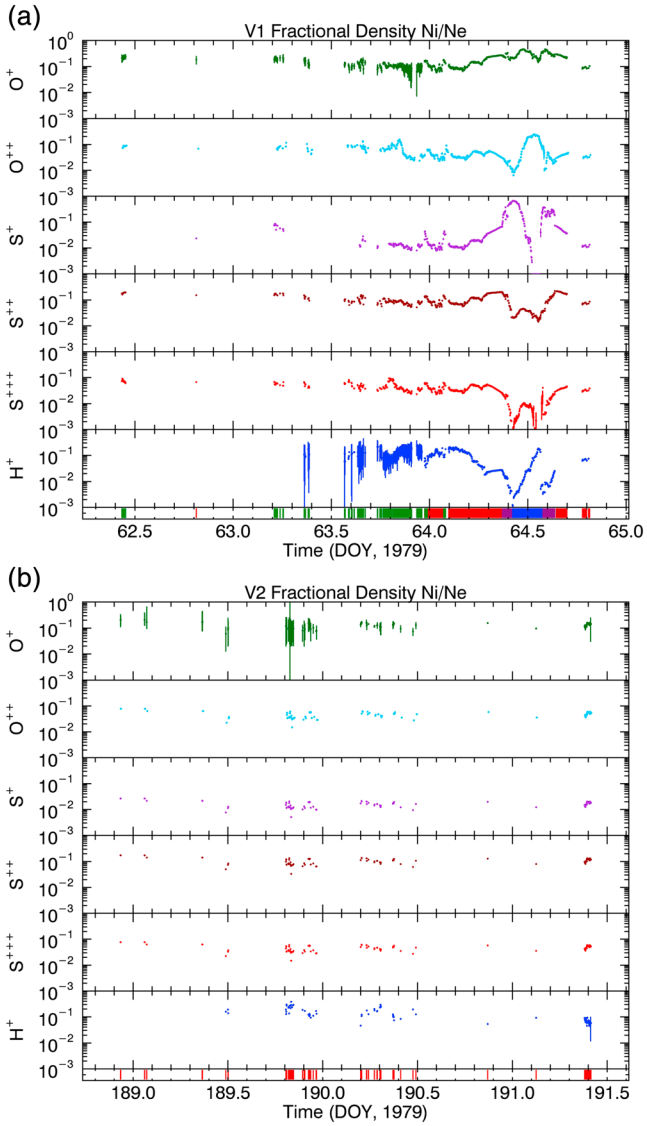

Figure 5. Ion composition derived from fitting (a) Voyager 1 and (b) Voyager 2 spectra. The colors in the bottom strip show the type of fit that was applied (case i in blue, case ii in red, case iii in purple, and case iv in green). For case ii (red) the composition was fixed to be that of the Delamere model so there are no error bars.

protons to keV levels, spreading the proton distribution to fit the noise signal. If the proton peak could be resolved, we let the code fit the peak; otherwise, we had to match the spectrum by eye. When the proton properties are specified rather than fitted the uncertainties in the proton density and temperature are not derived. The protons results are discussed further in paper 3.

3.3.4. Suprathermal Ions

Even in the very coldest regions of the Io plasma torus the Voyager PLS spectra show significant fluxes at higher energies, above the thermal component of the plasma. In the Io torus these suprathermal ions are probably recently ionized and retain some of the original pickup energy (540 eV for S^+ and 270 eV for O^+ at 6 R_J). Each ion species probably has a suprathermal component but without knowledge of the composition, we assumed that this hot component was O^+ throughout. In the inner torus (traversed only by Voyager 1) the suprathermal component can be well fit with a Maxwellian function (e.g., Figure 3a) suggestive of locally picked-up ions that have thermalized to a Maxwellian rather than retaining a ring beam or intermediate function as suggested by *Richardson and Siscoe* [1983b] and by *Smith and Strobel* [1985]. A separate Maxwellian at higher temperature (>100 eV) suggests that some combination of collisions and/or waves thermalizes the distribution before the ions fully equilibrate with the background plasma (at ~2 eV). Near the centrifugal equator the cold heavy ions dominate the density. But around closest approach (4.88 R_J) the Voyager 1 spacecraft was more than a couple scale heights below the centrifugal equator (see Figures 3 and 4 of *Bagenal* [1994]) so that the suprathermal component dominated the local density. It would be interesting to extend physical chemistry models to the cold torus [e.g., *Richardson et al.*, 1980; *Thomas et al.*, 2001; *Herbert et al.*, 2008] to explore the possible source and evolution of this suprathermal ion component.

Beyond about 5.7 R_J the suprathermal tail extends to higher energies resembling a power law tail (Figures 3b and 3c). These suprathermal tails to the ion distribution comprise just a few percent of the total plasma density in the warm torus, indicating that in this region of high density and slow radial transport the new pickup ions rapidly equilibrate with the surrounding plasma. Physical chemistry models of the torus also suggest that coulomb collisions bring the different ion species to similar temperatures (~100 eV) while maintaining the electrons at ~5 eV [*Delamere et al.,* 2005]. Meanwhile, the ~2 TW of UV radiation is the main heat sink for the torus.

Beyond ~8 R_J, particularly between cold blob regions, the suprathermal component comprises about half the charge density. Moreover, the suprathermal ions dominate the total plasma pressure [*McNutt,* 1983, 1984; *Mauk et al.,* 1996]. The suprathermal population was observed to extend into the energy range (>20 keV) of the Low-Energy Charged Particle Experiment (LECP) instrument on Voyager [*Krimigis et al*., 1981; *Mauk et al.,* 1996]. A proper analysis of these suprathermal tails will require combining these two data sets, perhaps fitting the combination with a kappa distribution function, in a future study.

3.4. Uncertainty in Fitted Parameters

In order to ascertain the uncertainties in the fitted parameters, we used an approach developed by *Wilson* [2015]. Using the curvature matrix of the parameters, and assuming a parabolic distribution in reduced chi-square near the minimum, it is possible to determine the 1σ uncertainty in the best fit parameter. Note that this method (and most others) does not allow for any interdependence between the parameters. For a full description of the error analysis method used in this study see online material "Voyager Plasma Science: Error Analysis." If these parameters were fixed (say, by the Delamere composition or at rigid corotation), then no error bars are shown in the parameter plots (Figures 4 and 5) discussed below. Table 1 lists the fit parameters and their percentage uncertainties. Again, because we ignore the interdependence of some of the parameters, these uncertainties are sometimes unrealistically small (especially when the peaks are not clearly resolved).

4. Results

Figures 4a and 4b show the net charge density, ion temperature, and azimuthal speed from fitting the Voyager 1 and Voyager 2 PLS spectra, respectively. Note that the colors in the strip at the bottom of each figure show the fitting cases applied at the corresponding time of the data. Blue corresponds to case i where the density of each ion species was allowed to vary independently. Red corresponds to case ii that was applied the region where the ion composition was fixed to that coming from the *Delamere et al.* [2005] model but the ion temperature and azimuthal speed allowed to vary. The case iii fits are shown in black, where both the composition and flow were fixed. Green corresponds to case iv, situations where the Delamere composition did not fit the data and the composition was adjusted by eye to match the spectra. The small region of purple corresponds to case v where the composition was interpolated between that of *Delamere et al.* [2005] at 6 R_J and the closest resolved spectrum inside at 5.3 R_J. For occasions where n, T_i, and V_φ were allowed to vary the error bars indicate the uncertainties in these parameters (shown with grey and blue vertical lines).

In the middle panels, the common ion temperature of all heavy ions is shown with black connected lines, while the proton temperature is shown in blue dots. The heavy ion temperatures tended to be somewhat higher for Voyager 2 than Voyager 1. The proton temperature tracks the heavy ion temperature quite closely for Voyager 1 and is lower for Voyager 2 (more consistent with the Voyager 1 values). Beyond about 10 R_J the temperature and density measured at the spacecraft exhibit significant rapid variations. The density and temperature are roughly anticorrelated with spectra in regions of high-density/colder plasma being easier to fit and the low-density/hotter plasma regions in between, sometimes sinking into the noise level of the PLS instrument.

As found in earlier studies [*McNutt et al.,* 1981; *Bagenal and Sullivan,* 1981] the azimuthal flow is close to rotation (shown by black curve in Figure 4) out to about 10 R_J, beyond which the corotation lag increases to an asymptotic azimuthal speed of about 220 km/s for Voyager 1 and 250 km/s for Voyager 2. In paper 2 we compare these radial profiles of corotation lag with predictions related to plasma mass loading and breakdown in coupling to the ionosphere.

Figures 5a and 5b show the ion composition from fitting Voyager 1 and Voyager 2 PLS spectra, respectively. The *Delamere et al.* [2005] composition fits the data reasonably well outside 6 R_J with some moderate exceptions that are discussed further in paper 2. At the same time, we recognize that we had to make substantial assumptions (common isotropic temperature, restricted composition, etc.) to fit these Voyager PLS data. It will be valuable to compare these ion compositions for the Voyager epoch with those obtained in similar regions of the plasma sheet by Juno which carries a plasma instrument with a time-of-flight measurement capability [*McComas et al*., 2013].

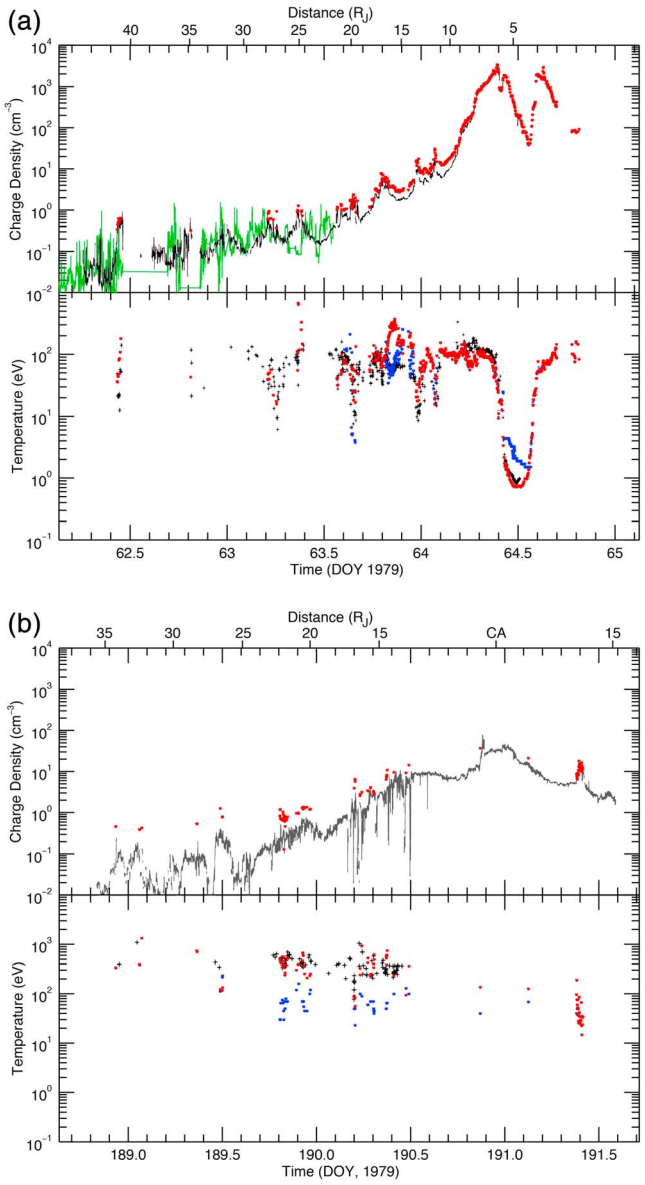

Figure 6. Comparison of total charge density and ion temperature from this study (red) via fitting spectra with values of these plasma parameters derived via numerical moments shown in black [*McNutt et al.*, 1981]. The blue dots are for proton temperatures. The green points are derived from the Voyager PWS instrument by *Barnhart et al.* [2009]. (a and b) Derived from Voyager 1 and Voyager 2 data, respectively.

Figures 6a and 6b compare the time profiles of density and temperature derived by this study via forward fitting of the PLS energy-per-charge spectra (shown in red for heavy ions and blue for protons) compared with density and temperature from the original analysis (black) presented by *McNutt et al.* [1981] and *Belcher* [1983]. Note that the ion temperature inside 9 R_J has been doubled from these original publications because of the revision reported by *Bagenal et al.* [1985].

As described in Appendix A of *McNutt et al.* [1981], when the plasma flow is sufficiently supersonic that the Faraday cups receive most of the flux and the thermal speed is sufficiently broader than the width of the energy channels, then the total charge density of the ions can be derived by summing the currents in the jth channels, I_j:

$$N_+ = n_j I_j / (e A_{\mathrm{eff}} V_n),$$

where e is the electron charge, A_{eff} is the effective area of the Faraday cup, and V_n is the component of the flow that is normal to the sensor. The black lines for density in top plots of Figures 6a and 6b are derived assuming V_n is the component of rigid corotation into the appropriate cup. There is an extensive discussion in *McNutt et al.* [1981] of how the fit values of density (red in Figures 6a and 6b) match the charge density from summation of currents because the lack of rigid corotation (which should increase the value of N_+) is compensated for by a lack of fitting the high-energy tail to the distribution. We argue that the contribution to the bulk density above the ~6 keV energy range of the Voyager PLS instrument is small (<10%), while the lack of corotation—particularly at earlier times and large distances—could explain why the numerically derived density (which assumes rigid corotation) is lower than the density derived from fits. Note that density can only be derived from fits to the spectra when the plasma is sufficiently cold and dense to produce spectral peaks. On the other hand, summation of the currents across the PLS energy range provides a reasonable estimate of the density even when the spectra are broad with no spectral peaks.

The local electron density can also be determined from the cutoff frequencies of various kinds of plasma waves observed in the frequency spectrum measured by an electric field instrument. *Barnhart et al.* [2009] carried out a survey of electron density derived from plasma wave (PWS) measurements from the Voyagers 1 and 2 passes through the Jovian magnetosphere and compared the values with the *McNutt et al.* [1981] densities. Note that the PWS measurements are limited by their frequency cutoff of 12 kHz.

Figure 6a shows that the Voyager 1 PWS (green) and PLS densities match reasonably well. The two data sets match with the PWS electron densities tending to be slightly higher than the numerical moments of *McNutt et al.* [1981], consistent with the electron densities derived from our forward modeling shown in Figure 6a.

The ion temperatures shown in Figure 6b come from fits to Voyager PLS spectra by *McNutt et al.* [1981]. The reason that there are relatively few points is that the plasma at the time of the Voyager 2 flyby was hotter and therefore less easy to analyze than for Voyager 1. During the Voyager 1 flyby there were well-determined temperatures in the cold torus (remembering that the original values of *Bagenal and Sullivan* [1981] needed to be multiplied by a factor of 2 as per *Bagenal et al.* [1985]). There were also several places in the plasma sheet ($>10\,R_J$) where the plasma was sufficiently cold that plasma parameters could be derived from fits to the energy-per-charge spectra. By assuming a composition—and sometimes also the azimuthal speed—it is possible to make an estimate of the temperature when the plasma is warmer, as illustrated by the warm temperatures exhibited by fits to the Voyager 2 data in this study. But there is still the limitation of the energy range of the instrument. Surveys of Galileo plasma data that extend up to energy-per-charge of 50 keV produce higher ion temperatures (by a factor of 5 to 10) at the same distance as Voyager beyond about $10\,R_J$ [*Frank and Paterson,* 2001; *Bagenal and Delamere,* 2011; *Bagenal et al.,* 2016]. Thus, the temperatures beyond ~$10\,R_J$ in Figure 6 should be taken as lower limits.

While the overall trends in density and temperature persist in Figure 6, it is interesting that there are places where the plasma varies quite rapidly over timescales of minutes. This is clear in the spectral plot of Figure 2a. Figures 5a and 6a show that around DOY 63.8 (or 63:1900) at a distance of about $17\,R_J$, the density, temperature, and composition all vary over tens of minutes. These cold blobs plus radial profiles of heavy ion parameters and protons are discussed further in papers 2 and 3, respectively.

5. Summary and Conclusions

This paper presents a survey of the Voyager PLS ion data obtained during the Voyager 1 and Voyager 2 passes through Jupiter's magnetosphere in 1979. We have archived the raw data, analysis programs, and output with full documentation. We summarize our findings from this reanalysis as follows:

1. The Voyager PLS ion data obtained in March and July 1979 in the magnetosphere of Jupiter remain valuable measurements of plasma parameters, particularly in regions of cold plasma inside $40\,R_J$. We focused on density, temperature, composition, and azimuthal flow in this paper. Analyses of nonazimuthal flows were presented by *McNutt et al.* [1981] and *Sands and McNutt* [1988].
2. For most of our analysis we fit the ion spectra assuming the ions have a common isotropic temperature (ranging from <1 eV to ~ keV). In the cold regions where ion spectral peaks can be fit separately this assumption seems to be reasonable. Physical chemistry models of the Io torus [*Smith and Strobel,* 1985; *Delamere et al.,* 2005] suggest that the lower ionization states (S^+, O^+) might have a somewhat higher (factor ~2) temperature than the other species (S^{++}, S^{+++}, and O^{++}) in the outer torus. Further complications arise due to a substantial suprathermal tail to the ion distributions. We were sometimes able to fit the tail with a comoving hot O^+ population, but we were limited by the 6 keV upper limit of the PLS instrument. A proper analysis would require simultaneously fitting data from both PLS and LECP Voyager instruments together with a kappa function. Moreover, one expects at least the suprathermal component to be anisotropic with respect to the magnetic field. Full analysis of the ion velocity distributions awaits data from the spinning Juno spacecraft with instrumentation that extends to higher energies and includes time-of-flight measurements [*McComas et al.,* 2013; *Mauk et al.,* 2013].
3. We find that we are able to fit the PLS spectra in the middle magnetosphere with a composition that is more or less consistent with that produced by the physical chemistry model of *Delamere et al.* [2005] with $S^+/Ne \sim 2$–3%, $S^{++}/Ne \sim 12$–16%, $S^{+++}/Ne \sim 5$–10%, $O^+/Ne \sim 15$–15%, $O^{++}/Ne \sim 9$–12%, and $\Sigma(O^{n+})/\Sigma(S^{n+}) \sim 0.8$, leaving about 10–15% of the charge as protons. Note that this composition was initially based on observations of the Io plasma torus by the Cassini UVIS instrument on its gravity assist flyby of Jupiter in 2000–2001. *Nerney et al.* [2017] recently reanalyzed the Voyager UV emissions from the Io torus and found that they could fit the spectra (using current atomic data) with a composition similar to the Cassini observations. A major difference between the recent *Nerney et al.* [2017] and the original *Shemansky* [1988] analyses is that the new study shows a much lower abundance of oxygen, particularly O^{++}. We further explore issues of the heavy ion composition in the accompanying paper 2.

4. The abundance of protons observed in the inner magnetosphere of Jupiter (near the equatorial plane) is consistently about 10% of the electron density. The locally measured proton composition drops in the cold inner torus, but this may be partly because the protons are forced off the equator by the ambipolar electric field. We further explore the distribution of protons as well as minor ions SO_2^+ and Na^+ in the accompanying paper 3.

Reanalysis of the Voyager PLS data has shown the measurements to be remarkably robust. Here we have presented the data as a function of time as the two Voyager spacecraft passed through the system. In the accompanying papers we extrapolate these observations along the magnetic field and compute integrated flux tube quantities that allow us to explore magnetospheric dynamics and comparisons between the two Voyager passes as well as with Galileo and Juno in situ plasma data.

Acknowledgments
The diligent archiving of PLS documentation by Ralph McNutt is gratefully appreciated. We thank Robert Wilson and Frank Crary for useful discussions. The raw Voyager PLS data are archived in the Planetary Data System (PDS—https://pds.nasa.gov/). The PWS densities came from the VG1-J-PWS-5-DDR-ELE-DENSITY-1S-V1.0 and VG2-J-PWS-5-DDR-PLASMA-DENSITY-1S-V1.0, data sets available at the PDS (https://pds.nasa.gov/). We have gathered the PLS data for the Jovian magnetosphere, the fitting routines, and output of our analysis here: http://lasp.colorado.edu/home/mop/missions/voyager. We acknowledge support from NASA's Jupiter Data Analysis Program (NNX09AE03G) as well as the Juno mission (SWRI subcontract 699050X).

References

Bagenal, F. (1985), Plasma conditions inside Io's orbit: Voyager measurements, *J. Geophys. Res.*, *90*, 311–324, doi:10.1029/JA090iA01p00311.
Bagenal, F. (1994), Empirical model of the Io plasma torus: Voyager measurements, *J. Geophys. Res.*, *99*, 11,043–11,062, doi:10.1029/93JA02908.
Bagenal, F., and J. D. Sullivan (1981), Direct plasma measurements in the Io torus and inner magnetosphere of Jupiter, *J. Geophys. Res.*, *86*, 8447–8466, doi:10.1029/JA086iA10p08447.
Bagenal, F., and P. A. Delamere (2011), Flow of mass and energy in the magnetospheres of Jupiter and Saturn, *J. Geophys. Res.*, *116,* A05209, doi:10.1029/2010JA016294.
Bagenal, F., J. D. Sullivan, and G. L. Siscoe (1980), Spatial distribution of plasma in the Io torus, *Geophys. Res. Lett.*, *7*, 41–44, doi:10.1029/GL007i001p00041.
Bagenal, F., R. L. McNutt Jr., J. W. Belcher, H. S. Bridge, and J. D. Sullivan (1985), Revised ion temperatures for Voyager plasma measurements in the Io plasma torus, *J. Geophys. Res.*, *90*, 1755–1757, doi:10.1029/JA090iA02p01755.
Bagenal, F., D. E. Shemansky, R. L. McNutt Jr., R. Schreier, and A. Eviatar (1992), The abundance of O^{++} in the Jovian magnetosphere, *Geophys. Res. Lett.*, *19*, 79–82, doi:10.1029/92GL00070.
Bagenal, F., et al. (2014), Magnetospheric science objectives of the Juno mission, *Space Sci. Rev.*, 1–69, doi:10.1007/s11214-014-0036-8.
Bagenal, F., R. J. Wilson, S. Siler, W. Paterson, and W. Kurth (2016), Survey of Galileo plasma observations in Jupiter's plasma sheet, *J. Geophys. Res. Planets*, *121*, 871–894, doi:10.1002/2016JE005009.
Barbosa, D. D. (1994), Neutral cloud theory of the Jovian nebula: anomalous ionization effect of suprathermal electrons, *Ap. J.*, *430*, 376–376, doi:10.1086/174413.
Barnett, A. (1986), In situ measurements of the plasma bulk velocity near the Io flux tube, *J. Geophys. Res.*, *91*, 3011–3019, doi:10.1029/JA091iA03p03011.
Barnett, A., and S. Olbert (1986), Response function of modulated grid Faraday cup plasma instruments, *Rev. Sci. Instrum.*, *57*, 2432–2440, doi:10.1063/1.1139089.
Barnhart, B. L., W. S. Kurth, J. B. Groene, J. B. Faden, O. Santolik, and D. A. Gurnett (2009), Electron densities in Jupiter's outer magnetosphere determined from Voyager 1 and 2 plasma wave spectra, *J. Geophys. Res.*, *114*, A05218, doi:10.1029/2009JA014069.
Belcher, J. W. (1983), The low-energy plasma in the Jovian magnetosphere, in *Physics of the Jovian Magnetosphere*, edited by A. J. Dessler, pp. 68–105, Cambridge Univ. Press, New York.
Belcher, J. W. (1987), The Jupiter-Io connection: An Alfvén engine in space, *Science*, *238*, 170–176, doi:10.1126/science.238.4824.170.
Belcher, J. W., and R. L. McNutt Jr. (1980), The dynamic expansion and contraction of the Jovian plasma sheet, *Nature*, *287*, 813–815, doi:10.1038/287813a0.
Belcher, J. W., C. K. Goertz, and H. S. Bridge (1980), The low energy plasma in the Jovian magnetosphere, *Geophys. Res. Lett.*, *7*, 17–20, doi:10.1029/GL007i001p00017.
Belcher, J. W., C. K. Goertz, J. D. Sullivan, and M. H. Acuna (1981), Plasma observations of the Alfvén wave generated by Io, *J. Geophys. Res.*, *86*, 8508–8512, doi:10.1029/JA086iA10p08508.
Bodisch, K. M., L. P. Dougherty, and F. Bagenal (2017), Survey of Voyager plasma science ions at Jupiter 3: Protons and minor ions, *J. Geophys. Res. Space Physics*, doi:10.1002/2017JA024148, in press.
Bridge, H. S., J. W. Belcher, R. J. Butler, A. J. Lazarus, A. M. Mavretic, J. D. Sullivan, G. L. Siscoe, and V. M. Vasyliunas (1977), The plasma experiment on the 1977 Voyager mission, *Space Sci. Rev.*, *21*, 259–287, doi:10.1007/BF00211542.
Bridge, H. S., et al. (1979a), Plasma observations near Jupiter: Initial results from Voyager 1, *Science*, *204*, 987–991, doi:10.1126/science.204.4396.987.
Bridge, H. S., et al. (1979b), Plasma observations near Jupiter: Initial results from Voyager 2, *Science*, *206*, 972–976, doi:10.1126/science.206.4421.972.
Broadfoot, A. L., et al. (1979), Extreme ultraviolet observations from Voyager I encounter with Jupiter, *Science*, *204*, 979–982, doi:10.1126/science.204.4396.979.
Burlaga, L. F., J. W. Belcher, and N. F. Ness (1980), Disturbances observed near Ganymede by Voyager 2, *Geophys. Res. Lett.*, *7*, 21–24, doi:10.1029/GL007i001p00021.
Delamere, P., F. Bagenal, and A. Steffl (2005), Radial variations in the Io plasma torus during the Cassini era, *J. Geophys. Res.*, *110*, A12223, doi:10.1029/2005JA011251.
Dougherty, L. P., K. M. Bodisch, and F. Bagenal (2017), Survey of Voyager plasma science ions at Jupiter 2: Heavy ions, *J. Geophys. Res. Space Physics*, doi:10.1002/2017JA024053, in press.
Frank, L. A., and W. R. Paterson (2001), Survey of thermal ions in the Io plasma torus with the Galileo spacecraft, *J. Geophys. Res.*, *106*, 6131–6149, doi:10.1029/2000JA000159.
Frank, L. A., K. L. Ackerson, J. A. Lee, M. R. English, and G. L. Pickett (1992), The plasma instrumentation for the Galileo mission, *Space Sci. Rev.*, *60*, 283–307, doi:10.1007/BF00216858.

Herbert, F., N. M. Schneider, and A. J. Dessler (2008), A new description of Io's cold plasma torus, *J. Geophys. Res.*, *113*, A01208, doi:10.1029/2007JA012555.
Khurana, K., M. G. Kivelson, V. Vasyliunas, N. Krupp, J. Woch, A. Lagg, B. Mauk, and W. Kurth (2004), The configuration of Jupiter's magnetosphere, in *Jupiter: Planet, Satellites, Magnetosphere*, edited by F. Bagenal, T. E. Dowling, and W. B. McKinnon, Cambridge Univ. Press, Cambridge, U. K.
Krimigis, S. M., J. F. Carbary, E. P. Keath, C. O. Bostrom, W. I. Axford, G. Gloeckler, L. J. Lanzerotti, and T. P. Armstrong (1981), Characteristics of hot plasma in the Jovian magnetosphere: Results from the Voyager spacecraft, *J. Geophys. Res.*, *86*, 8227, doi:10.1029/JA086iA10p08227.
Krupp, N., et al. (2004), Dynamics of the Jovian magnetosphere, in *Jupiter: Planet, Satellites, Magnetosphere*, edited by F. Bagenal, T. E. Dowling, and W. B. McKinnon, Cambridge Univ. Press, Cambridge, U. K.
Markwardt, C. B. (2009), Non-linear least squares fitting in IDL with MPFIT, in *Proceedings of Astronomical Data Analysis Software and Systems XVIII, Quebec, Canada, ASP Conference Series*, vol. 411, edited by D. Bohlender, P. Dowler, and D. Durand, pp. 251–254, Astron. Soc. of the Pacific, San Francisco, Calif.
Mauk, B. H., S. A. Gary, M. Kane, E. P. Keath, and S. M. Krimigis (1996), Hot plasma parameters of Jupiter's inner magnetosphere, *J. Geophys. Res.*, *101*, 7685–7695, doi:10.1029/96JA00006.
Mauk, B. H., et al. (2013), The Jupiter Energetic Particle Detector Instrument (JEDI) investigation for the Juno mission, *Space Sci. Rev.*, 1–58, doi:10.1007/s11214-013-0025-3.
McComas, D. J., et al. (2013), The Jovian Auroral Distributions Experiment (JADE) on the Juno mission to Jupiter, *Space Sci. Rev.*, 1–97, doi:10.1007/s11214-013-9990-9.
McNutt, R. L., Jr. (1983), Force balance in the magnetospheres of Jupiter and Saturn, *Adv. Space Res.*, *3*, 55–58, doi:10.1016/0273-1177(83)90256-9.
McNutt, R. L., Jr. (1984), Force balance in outer planet magnetospheres, *Phys. Space Plasmas*, *5*, 179–210.
McNutt, R. L., Jr., J. W. Blecher, J. D. Sullivan, F. Bagenal, and H. S. Bridge (1979), Departure from rigid co-rotation of plasma in Jupiter's dayside magnetosphere, *Nature*, *280*, 803, doi:10.1038/280803a0.
McNutt, R. L., Jr., J. W. Belcher, and S. H. Bridge (1981), Positive ion observations in the middle magnetosphere of Jupiter, *J. Geophys. Res.*, *86*, 8319–8342, doi:10.1029/JA086iA10p08319.
McNutt, R. L., Jr., P. S. Coppi, R. S. Selesnick, and B. Coppi (1987), Plasma depletions in the Jovian magnetosphere: Evidence of transport and solar wind interaction, *J. Geophys. Res.*, *92*, 4377–4398, doi:10.1029/JA092iA05p04377.
McNutt, R. L., Jr., F. Bagenal, and R. M. Thorne (1990), Observation of auroral secondary electrons in the Jovian magnetosphere, *Geophys. Res. Lett.*, *17*, 291–294, doi:10.1029/GL017i003p00291.
Moreno, M. A., W. I. Newman, and M. G. Kivelson (1985), Ion partitioning in the hot Io torus: Influence of S2 outgassing, *J. Geophys. Res.*, *90*, 12,065–16,072, doi:10.1029/JA090iA12p12065.
Nerney, E., F. Bagenal, and A. Steffl (2017), Io plasma torus ion composition: Voyager, Galileo, Cassini, *J. Geophys. Res. Space Physics*, *122*, 727–744, doi:10.1002/2016JA023306.
Pontius, D. H., Jr., T. W. Hill, and M. E. Rassbach (1986), Steady state plasma transport in a corotation dominated magnetosphere, *Geophys. Res. Letts.*, *11*, 1097–1100, doi:10.1029/GL013i011p01097.
Richardson, J. D., and G. L. Siscoe (1981), Factors governing the ratio of inward to outward diffusing flux of satellite ions, *J. Geophys. Res.*, *86*, 8485–8490, doi:10.1029/JA086iA10p08485.
Richardson, J. D., and G. L. Siscoe (1983a), The problem of cooling the cold Io torus, *J. Geophys. Res.*, *88*, 2001–2009, doi:10.1029/JA088iA03p02001.
Richardson, J. D., and G. L. Siscoe (1983b), The non-Maxwellian energy distribution of ions in the warm torus, *J. Geophys. Res.*, *88*, 8097–8102, doi:10.1029/JA088iA10p08097.
Richardson, J. D., and R. L. McNutt Jr. (1987), Observational constraints on interchange models at Jupiter, *Geophys. Res. Lett.*, *14*, 64–67, doi:10.1029/GL014i001p00064.
Richardson, J. D., G. L. Siscoe, F. Bagenal, and J. D. Sullivan (1980), Time dependent plasma injection by Io, *Geophys. Res. Lett.*, *7*, 37–40, doi:10.1029/GL007i001p00037.
Sands, M. R., and R. L. McNutt Jr. (1988), Plasma bulk flow in Jupiter's dayside middle magnetosphere, *J. Geophys. Res.*, *93*, 8502–8518, doi:10.1029/JA093iA08p08502.
Scudder, J. D., E. C. Sittler Jr., and H. S. Bridge (1981), A survey of the plasma electron environment of Jupiter: A view from Voyager, *J. Geophys. Res.*, *86*, 8157–8179, doi:10.1029/JA086iA10p08157.
Shemansky, D. E. (1988), Energy branching in the Io plasma torus: The failure of neutral cloud theory, *J. Geophys. Res.*, *93*, 1773–1784, doi:10.1029/JA093iA03p01773.
Sittler, E. C., Jr., and D. F. Strobel (1987), Io plasma torus electrons: Voyager 1, *J. Geophys. Res.*, *92*, 5741–5762, doi:10.1029/JA092iA06p05741.
Smith, R. A., and D. F. Strobel (1985), Energy partitioning in the Io plasma torus, *J. Geophys. Res.*, *90*, 9469–9493, doi:10.1029/JA090iA10p09469.
Steffl, A. J., F. Bagenal, and A. I. F. Stewart (2004a), Cassini UVIS observations of the Io plasma torus: I. Initial results, *Icarus*, *172*, 78–90, doi:10.1016/j.icarus.2003.12.027.
Steffl, A. J., F. Bagenal, and A. I. F. Stewart (2004b), Cassini UVIS observations of the Io plasma torus: II. Radial variations, *Icarus*, *172*, 91–103, doi:10.1016/j.icarus.2004.04.016.
Sullivan, J. D., and F. Bagenal (1979), In situ identification of various ionic species in Jupiter's magnetosphere, *Nature*, *280*, 798–799, doi:10.1038/280798a0.
Summers, D., and G. L. Siscoe (1985), Wave modes of the Io plasma torus, *Astrophys. J.*, *295*, 678–684, doi:10.1086/163411.
Thomas, N., G. Lichtenberg, and M. Scotto (2001), High-resolution spectroscopy of the Io plasma torus during the Galileo mission, *J. Geophys. Res.*, *106*, 26,277–26,291, doi:10.1029/2000JA002504.
Thomas, N., F. Bagenal, T. Hill, and J. Wilson (2004), The Io neutral clouds and plasma torus, in *Jupiter: Planet, Satellites, Magnetosphere*, edited by F. Bagenal, T. E. Dowling, and W. B. McKinnon, Cambridge Univ. Press, Cambridge, U. K.
Wilson, R. J. (2015), Error analysis for numerical estimates of space plasma parameters, *Earth Space Sci.*, *2*, 201–222, doi:10.1002/2014EA000090.